

Procedure to Estimate the Crack Resistance Curve from the Instrumented Charpy V–Notched Impact Test

R. Chaouadi^{a,†} and J.L. Puzzolante^b

^b *SCK•CEN, Boeretang 200, 2400 Mol, Belgium*

Abstract

Recently, a simple procedure based on the relationship between crack length and absorbed energy was provided to determine the crack length from the load–displacement test record. This procedure was validated on a large number of materials using various cracked geometries. The main objective of this paper is to investigate the possibility to apply a similar procedure to a V–notched geometry, namely the Charpy specimen. Such an evaluation would lead to estimate the material crack resistance from a single Charpy V–notched impact test.

By performing a number of well–selected experiments, we demonstrated that such a correlation exists, allowing the determination of both static as well as dynamic (impact) crack resistance from the simple instrumented Charpy impact test with a reasonable accuracy.

Keywords: ductile fracture, crack resistance, Charpy V–notched, quasi–static loading, dynamic loading

1. Introduction

The Charpy impact test is one of the reference tests used to determine the fracture resistance of structural steels. Many engineers and scientists investigated the possibility to correlate Charpy impact energy with the fracture toughness. Indeed, the Charpy impact test is considered as a cheap and easy test in comparison to the fracture toughness test which requires precracking and more sophisticated instrumentation to monitor crack extension. As a result, many empirical correlations were proposed in literature [1–8]. However, most of these correlations are limited in terms of range of application due primarily to their empirical basis. These correlations were mainly established on the basis of experimental data including Charpy impact energy, static fracture toughness and static yield strength, lumping therefore effects related to loading rate, notch acuity and crack length–to–width ratio.

Recently, a simple procedure was provided to determine crack length from the load–displacement test record [9]. The basic underlying idea is that crack length is proportional to the square of absorbed energy. This procedure was validated on a large number of materials using various cracked geometries. It was also demonstrated to be applicable to shallow crack configurations, to large crack extensions [9, 10] as well as impact–loaded tests [11]. The main objective of this paper is to investigate the possibility to apply a similar procedure to a V–notched

[†] corresponding author: Tel: +32-14-333176 ; Fax: +32-14-321216 Email address: rachid.chaouadi@sckcen.be.

geometry, namely the Charpy V-notched specimen, to determine the quasi-static crack resistance. Three effects must be considered:

- Effect of the notch/crack acuity: in the Charpy impact specimen, the V-notch radius is 0.25 mm, which is significantly larger than the infinitely small crack tip radius;
- Effect of the notch/crack depth-to-width ratio: in the Charpy impact specimen, the notch depth-to-width ratio is 0.2 while it is close to 0.5 for fracture mechanics specimens;
- Effect of the loading rate: the Charpy impact test is dynamic while fracture mechanics tests are measured under quasi-static loading.

In order to consider these effects, we performed a number of dedicated tests to derive their individual contributions. In the following, the energy normalization procedure will be briefly recalled and additional information on how it can be applied to the instrumented Charpy impact test will be given.

2. Crack resistance determination procedure from the single Charpy V-notched sample

The crack resistance behavior is obtained using the following procedure. As more details can be found in [9, 11], only the necessary elements are given here. The J-integral calculation is based on the ASTM standard [12], which, for the single edge bend geometry, gives the following equation:

$$J_{(i)} = \frac{K_{(i)}^2(1-\nu^2)}{E} + \left[J_{pl(i-1)} + \frac{\eta}{W - a_{(i-1)}} \frac{U_{pl(i)} - U_{pl(i-1)}}{B_n} \right] \left(1 - \frac{a_{(i)} - a_{(i-1)}}{W - a_{(i-1)}} \right) \quad (1)$$

where U_{pl} is the area under the load-displacement curve (the plastic part, only), W , B_n and a are the specimen width, net thickness and crack length, respectively, K is the stress intensity factor (linear elastic) and (i) is the increment. E is the Young's modulus and ν is the Poisson's ratio.

As can be seen, in equation (1), the J-integral is incrementally evaluated using the actual crack length. It was shown in [9] that the crack extension could be estimated from the absorbed energy (area under the load-displacement test record, U). The crack extension can be calculated using equation (2):

$$\Delta a_{(i)} \approx \Delta a_{final} \left(\frac{U_{(i)} - U_{init}}{U_{final} - U_{init}} \right)^2 = \Delta a_{final} \left(\frac{J_{(i)} - J_{init}}{J_{final} - J_{init}} \right)^2 \quad (2)$$

Calculation of crack growth is performed in two steps. Indeed, to evaluate the J-integral according to equation (1), the crack length is required. First, the crack extension is first *approximately* estimated using equation (2) left hand where U_{init} is the energy required for crack growth onset. As it will be seen later, this threshold value corresponds to the onset of ductile crack initiation. Below this energy, no crack extension occurs, and therefore, $\Delta a=0$ if $U < U_{init}$. Once J-values are calculated, the actual crack extension is re-calculated using equation (2) right hand.

This procedure assumes that onset of crack initiation occurs at a load between the general yield (linear part) and the maximum load carrying capacity [11], or in terms of characteristic forces:

$$F_{init} \approx \frac{F_{gy} + F_{max}}{2} \quad (3)$$

where F_{gy} and F_{max} are the general yield and maximum loads (see Figure 1).

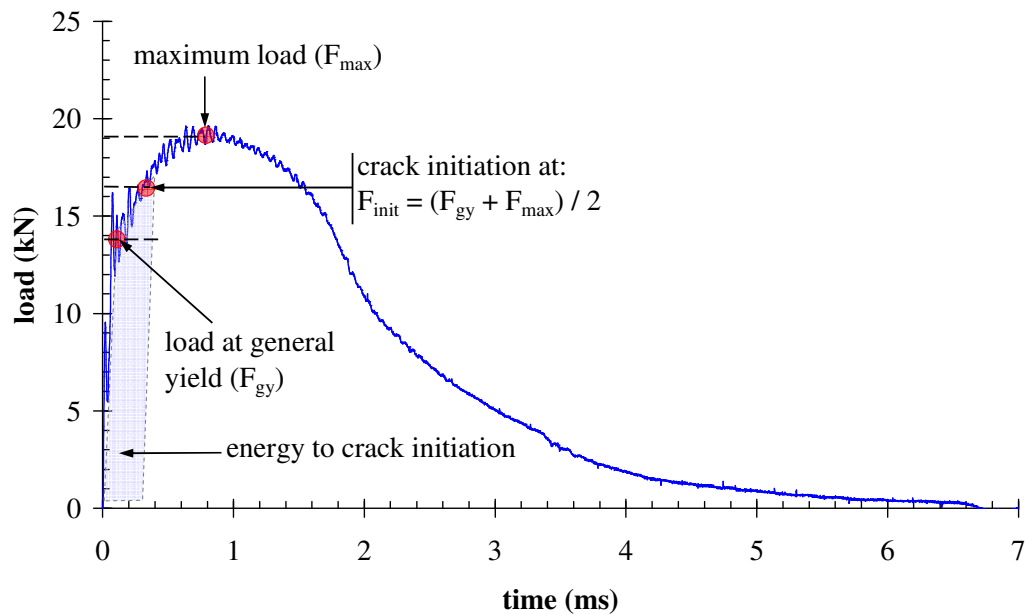


Figure 1. Typical load – time test record of Charpy impact test indicating some characteristic points.

This relation stems from the correlation between the shear fracture appearance and the characteristic loads of an instrumented Charpy impact test [11, 13, 14]. It was experimentally verified using various techniques [15–17] that crack initiation occurs at a load according to equation (3). Moreover, for cracked specimens, equation (3) was found to lead to a very good agreement with the unloading compliance method [9] while other relations, such as crack initiation at maximum load, clearly deteriorate this agreement [11].

This procedure for crack resistance determination was extensively verified on a number of materials, geometries and experimental conditions [9–11]. Compared to other normalization procedures, such as the one proposed in the ASTM standard [12], this one is more closely based on the actual response of the material and applicable to specimens fully broken.

The same procedure can be applied to the notched rather than cracked geometry, namely the Charpy V-notched sample under impact loading. However, a number of data manipulations are needed to be able to calculate the J-integral.

To determine the area under the load–displacement curve, as specified by equations (1) and (2), the displacement, $s(t)$, should be calculated using the following equation:

$$s(t) = \int_{t_0}^t v(t) dt \quad (4)$$

where $v(t)$ is the actual velocity of the impact hammer given by:

$$v(t) = v_0 - \frac{1}{m} \int_{t_0}^t F(t) dt \quad (5)$$

v_0 and m are the initial velocity and the mass of the impact hammer, respectively, $F(t)$ is the load at time t .

The absorbed energy, $U_{(i)}$, can then easily be calculated using equation (6):

$$U_{(i)} = \int_0^{s_{(i)}} F ds \quad (6)$$

For the J–integral calculation, the same formulation as equation (1) is used except that the factor η is not constant (as in deeply notched samples), but changes with the crack configuration. Indeed, for a shallow crack, this factor was found to depend much on the crack length–to–width ratio and the following formulation, due to Sumpter [18] was adopted here:

$$\left\{ \begin{array}{ll} \eta = 0.32 + 12 \left(\frac{a}{W} \right) - 49.5 \left(\frac{a}{W} \right)^2 + 99.8 \left(\frac{a}{W} \right)^3 & \frac{a}{W} < 0.268 \\ \eta = 1.9 & \frac{a}{W} \geq 0.268 \end{array} \right. \quad (7)$$

The original value of η for deep cracks was 2 and the a/W –transition was 0.282. These two values were updated in equation (7) to comply with the last updates of the ASTM 1820 standard [12]. Note that other formulations of the η –factor can be found in literature [19, 20]. However, the observed differences are relatively small and well below the usual experimental scatter bands.

Combining equation (1) and (7), the J–integral value can be evaluated at each data point. However, in the incremental J–formulation, equation (1), the crack growth correction is not applicable for very large crack extensions. Indeed, above a certain crack extension, corresponding approximately to a crack length–to–width ratio of about 0.75, the J–integral as calculated from equation (1) leads to J–values decreasing with crack length. In a Charpy impact test, the location of such a turning point corresponds to the onset of shear lip formation. Because crack extension is calculated according to equation (2), this leads to abnormal values. Of course, for such high crack extensions, the J–integral concept becomes invalid. However, as will be seen later, a good approximation of the crack resistance curve can still be obtained. It should be emphasized here that the aim of the present paper is to provide a good estimate of the crack resistance from a single Charpy impact test.

3. Experimental

Two reactor pressure vessel steels, 20MnMoNi55 forging and A533B (JSPS) plate, that were extensively investigated at SCK•CEN [11, 14] were selected for the present investigation. These materials and the test temperature conditions provide a wide range of crack resistance behaviors. As a result, the materials and test temperatures were selected such that three very distinct crack resistance curves could be obtained [11].

All fracture tests performed here use the Charpy geometry. The standard Charpy specimen, referred to as CVN, is the standard Charpy specimen with a 45° V-notch of 2 mm depth. The samples that were fatigue precracked refer to as PCCv. For the quasi-static tests, the specimens were loaded in three-point bending on an electromechanically driven testing machine with a slow displacement rate (few tenths of mm/min). For the dynamic tests, the Charpy impact test machine was used, the available impact energy being adapted to produce the desired crack length. The J-rate corresponds approximately to $\sim 1 \text{ kJ.m}^{-2}.\text{s}^{-1}$ for the quasi-static tests and to $\sim 10^5 \text{ kJ.m}^{-2}.\text{s}^{-1}$ for the dynamic tests. Further details on the experimental procedure can be found in [11].

To reduce the size of the test matrix, the tests were selected such as to provide separate effects of each variable with the ultimate goal to provide the crack resistance from the CVN impact test. Details can be found elsewhere [21].

4. Results, Analysis and Interpretation

First, it is important to confirm the loading rate effect on the Charpy V-notched geometry. Indeed, in the case of precracked Charpy specimens with $a/W \approx 0.5$, it was shown in [11] that there is a proportionality between quasi-static and dynamic crack resistance curves, such as:

$$J_R^{static} = \alpha_{loading\ rate} \times \left(\frac{\sigma_y^{dynamic}}{\sigma_y^{static}} \right)^2 \times J_R^{dynamic} \quad (8)$$

where the constant $\alpha_{loading\ rate}$ approximately equals 0.46 and σ_y^{static} and $\sigma_y^{dynamic}$ are the static and dynamic yield strengths.

This equation, denoting the effect of loading rate on the loss of crack tip constraint, was obtained with deeply cracked samples ($a/W \approx 0.5$). For shallow cracks, it is known that an apparent crack resistance elevation is observed because of loss of crack tip constraint [22]. By performing Charpy V-notched tests at two loading rates, quasi-static and impact, the same relation is found still applicable for the V-notched geometry [21]. The significant effect is attributed to the crack length-to-width ratio, a/W , which affects the crack tip constraint. We adopted the same strategy as for the loading rate effect by introducing a factor that accounts for the crack configuration effect (deep crack versus shallow notch). Similarly as equation (8), one can write:

$$J_R^{deep\ crack} = \beta_{crack\ configuration} \times J_R^{shallow\ notch} \quad (9)$$

where $\beta_{crack\ configuration}$ accounts for the loss of constraint introduced by the specimen configuration, more precisely the shallow crack versus deep crack configuration.

Because of crack blunting phenomenon that occurs before fracture initiation, the notch acuity (notch versus crack) has only a negligible effect on the crack resistance behavior and this was experimentally verified in [21].

Combining equations (8) and (9), one obtains the relation allowing determination of the static crack resistance from the Charpy impact test:

$$J_R^{static} = \alpha_{loading\ rate} \times \beta_{crack\ configuration} \times \left(\frac{\sigma_y^{dynamic}}{\sigma_y^{static}} \right)^2 \times J_R^{CVN\ impact} \quad (10)$$

To obtain the dynamic crack resistance, equation (10) reduces to:

$$J_R^{dynamic} = \beta_{crack\ configuration} \times J_R^{CVN\ impact} \quad (11)$$

$J_R^{CVN\ impact}$ corresponds to the crack resistance curve based on the standard Charpy specimen. It can be calculated using equations (1), (2) and (7). So, equations (10) and (11) can be used to estimate both the static and dynamic crack resistance curves from the Charpy impact test.

Using the available experimental results, we tentatively tried to determine the factor $\beta_{crack\ configuration}$ that rationalizes all results. However, it was not possible to rationalizing all experimental result with a unique factor, but this factor seems to depend on the loading rate as well, namely $\beta_{crack\ configuration} = 0.52$ at quasi-static loading rate and $\beta_{crack\ configuration} = 0.84$ at impact loading rate. It is important to note that, at quasi-static loading rate, the value obtained here is in close agreement with the ratio of the J_R -curve obtained with $a/W=0.6$ and $a/W=0.1$, namely ~ 0.6 [22]. The test results obtained with the Charpy V-notched specimen geometry shown in Figure 2 lead to a good agreement considering equation (10).

If we consider the following tests:

1. CVN ($a/W=0.2$) multiple specimen tests under static loading;
2. CVN ($a/W=0.2$) single fully broken test under impact loading;
3. PCCv ($a/W\approx 0.5$) multiple specimen tests under impact loading;
4. PCCv ($a/W\approx 0.5$) single specimen test under static loading;

Figure 3 shows that all these data can be rationalized using equation (10). The agreement between the various tests is reasonably good. This Figure clearly supports the capability of determining both the static and dynamic crack resistance curves from a single instrumented Charpy V-notched impact test.

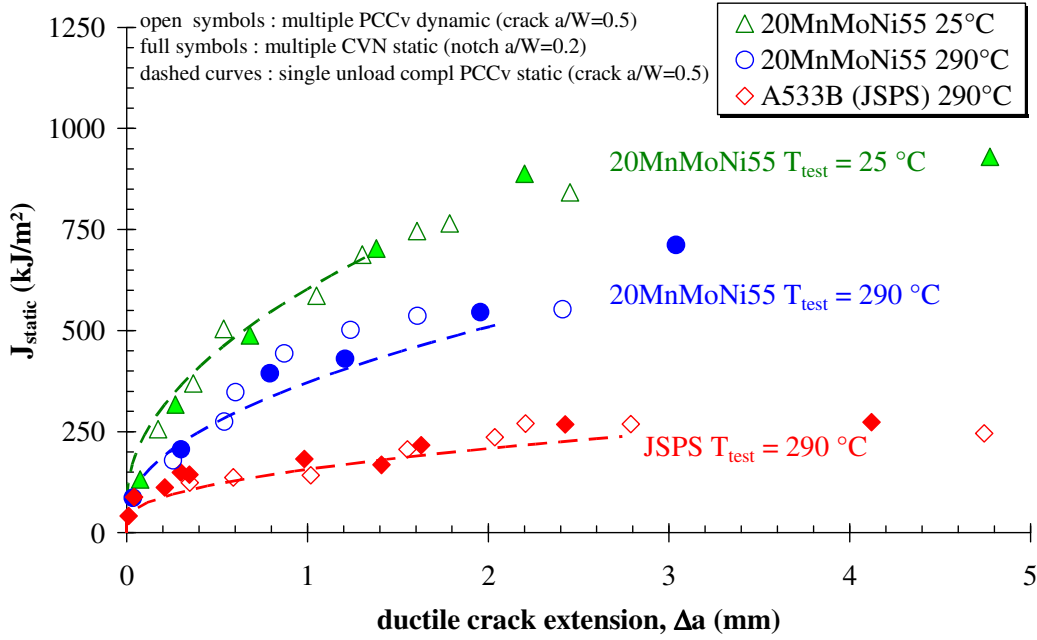


Figure 2. Crack resistance curves as derived from the static Charpy V-notch geometry, accounting for the crack configuration effect through $\beta_{crack\ configuration}=0.52$.

There are limitations of the procedure presented here, in particular the application of equation (10). These restrictions are mainly related to the constants accounting for notch/crack configuration and loading rate effects. These constants were empirically established based on experimental results. Therefore, application to other material and experimental conditions will probably need re-evaluation of these constants. Because these constants were introduced to account for the loss of constraint, it will be very interesting and desirable to relate them directly to the actual loss of constraint calculations using finite element computations. A number of such calculations were already published to evaluate the loss of constraint induced by crack configuration and loading rate, for example [23, 24]. Analytical expressions can then be established based on the finite element results of the form:

$$\omega_{loss\ of\ constraint} = \alpha_{loading\ rate} \times \beta_{crack\ configuration} = f\left(\frac{\sigma_y}{E}, \frac{d\varepsilon}{dt}, n, \frac{a}{W}, \frac{dJ}{dt}\right) \quad (12)$$

where all important parameters related to material, crack configuration and loading rate are taken into account. Equation (12) can then be fitted to the finite element results.

Note that in this work, all specimens were plain sided (not side grooved). In presence of side grooves, the change of loss of constraint factor should also be taken into account.

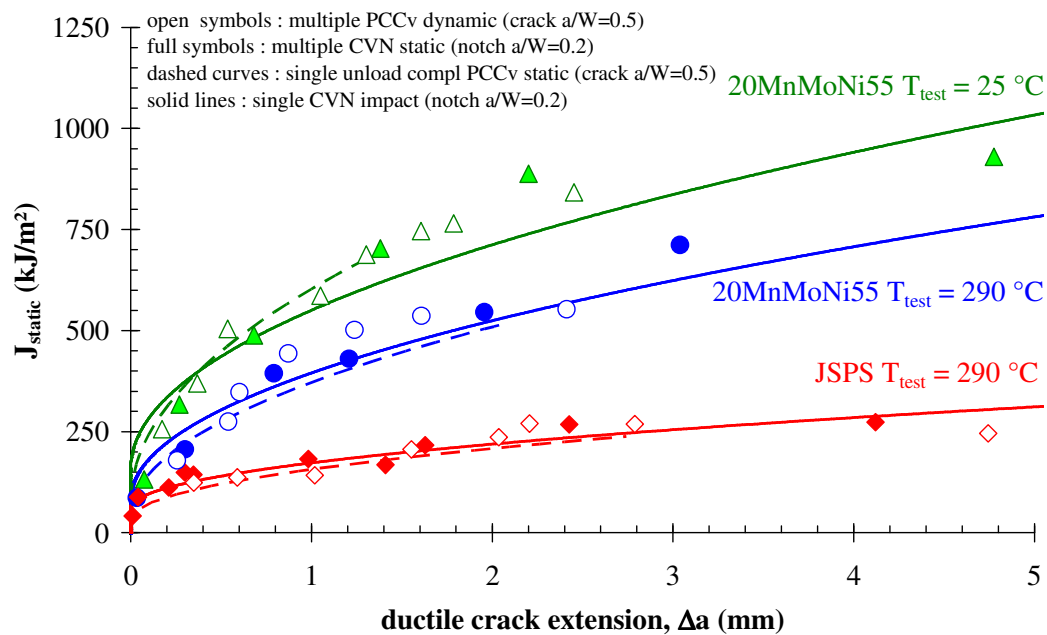


Figure 3. Summary of the various crack resistance curves of 20MnMoNi55 and A533B (JSPS).

5. Conclusions

This study has demonstrated the possibility to reasonably estimate the crack resistance behavior from the instrumented Charpy impact test. The procedure is solely based on the instrumented Charpy impact test record. Both dynamic and static crack resistance can be derived with a reasonably good accuracy. Test temperature and loading rate effects are taken into account through the constants introduced to account for the loss of constraint and the loading rate effect on the yield strength. These constants were experimentally determined for the material, specimen configuration and loading rate conditions investigated here. But, to increase the range of application, a better account of these effects would be possible by performing appropriate finite element calculations to analytically express the constants as a function of crack depth-to-width ratio and loss of triaxiality.

Acknowledgments

The authors gratefully acknowledge the technical support of R. Mertens, A. Pellettieri and L. Van Houdt. The steels, 20MnMoNi55 and A533B (JSPS) were kindly provided by J. Heerens (GKSS) and K. Onizawa (JAEA), respectively. Many thanks to J. Wagemans for reviewing of the paper.

References

- [1] S.T. Rolfe, J.M. Barsom, *Fracture and Fatigue Control in Structure – Application of Fracture Mechanics*, Prentice–Hall, Inc., Englewood Cliffs, New Jersey, 1977.

- [2] S.T. Rolfe, S.R. Novak, Slow-bend K_{Ic} testing of medium-strength high-toughness steels, in: Review of Development in Plane Strain Fracture Toughness Testing, ASTM STP 463, 1970, pp. 124–159.
- [3] J.M. Barsom, S.T. Rolfe, Correlation between K_{Ic} and Charpy V-notch test results in the transition temperature range, in: Impact Testing of Metals, ASTM STP 466, 1970, pp. 281–302.
- [4] H.G. Pisarski, A review of correlations relating Charpy energy to K_{Ic} , The Welding Inst Res Bulletin, 12 (1978) 362–367.
- [5] B. Nageswara Rao, A.R. Acharya, A computer study on evaluation of fracture toughness from Charpy V-notch impact energy and reduction of area, Eng Frac Mech 41 (1992) 85–90.
- [6] H.J. Schindler, Relation between fracture toughness and Charpy fracture energy: an analytical approach, in: T.A. Siewert, M.P. Manahan (Eds.), Pendulum Impact Testing: A Century of Progress, ASTM STP 1380, 2000, pp. 337–353.
- [7] P.C. Gioielli, J.D. Landes, J.D. Paris, H. Tada, L. Loushin, Method for predicting J–R curves from Charpy impact energy, in: P.C. Paris, K.L. Jerina (Eds.) Fatigue and Fracture Mechanics: 30th Volume, ASTM STP 1360, 2000, pp. 61–68.
- [8] K. Wallin, Low cost J–R curve estimation based on CVN upper shelf energy, Fat Frac Eng Mat Struc 24 (2001) 537–549.
- [9] R. Chaouadi, An energy-based crack extension formulation for crack resistance characterization of ductile materials, J Test Eval 32 (2004) 469–475.
- [10] R. Chaouadi, Crack resistance determination from the load–displacement test record, SCK•CEN Report R–3712, 2003.
- [11] R. Chaouadi, J.L. Puzzolante, Loading rate effect on ductile crack resistance of steels using precracked Charpy specimens, Int J Press Vess Piping 85 (2008) 752–761.
- [12] ASTM, E 1820–08, Standard Test Method for Measurement of Fracture Toughness, Annual Book of ASTM Standards, Section III, Metals Test Methods and Analytical Procedures, Vol. 03.01, American Society for Testing and Materials (2008).
- [13] A. Fabry, E. van Walle E, J. Van de Velde, R. Chaouadi, J.L. Puzzolante, T. van Ransbeeck, A. Verstrepen, On the use of the instrumented Charpy V impact signal for assessment of RPVS embrittlement, in: van Walle E (Ed.) Evaluating Material Properties by Dynamic Testing ESIS Publication 20, 1996, pp. 59–78.
- [14] R. Chaouadi, A. Fabry, On the utilization of the instrumented Charpy impact test for characterizing the flow and fracture behavior of reactor pressure vessel steels, in: D. François, A. Pineau (Eds.), From Charpy to Present Impact Testing, Elsevier, 2002, pp. 103–117.

- [15] A. Fabry, E. van Walle, R. Chaouadi, J.P. Wannijn, A. Verstrepen, J.L. Puzzolante, T. van Ransbeeck, J. Van de Velde J, RPV steel embrittlement – Damage modeling and micromechanics, SCK•CEN Report BLG–649, 1993.
- [16] H.W. Viehrig, J. Boehmert, H. Richter, M. Valo, Use of instrumented Charpy test for determination of crack initiation toughness, in: T.A. Siewert, M.P. Manahan (Eds.) Pendulum Impact Testing: A Century of Progress, ASTM STP 1380, 2000, pp. 354–365.
- [17] G.B. Lenkey, L. Toth, Measurement techniques for determination of ductile crack initiation on Charpy specimens, *Materialwiss Werkstofftech* 32 (2001) 562–567.
- [18] J.D.G. Sumpter, J_c -determination for shallow notch welded bend specimens, *Fat Frac Eng Mat Struc* 10 (1987) 479–493.
- [19] M. Nevalainen, K. Wallin, The effect of crack depth and absolute thickness on fracture toughness of 3PB specimens, in: K.H. Schwalbe, C. Berger (Eds.) Proceedings of the 10th European Conference on Fracture, ECF–10, Structural Integrity: Experiments, Models and Applications, Vol. II, 1994, pp. 997–1006.
- [20] P.R. Sreenivasan, S.L. Mannan, Plastic η -factor for three-point bend specimens: Analysis of instrumented Charpy impact test results for AISI 308 weld and AISI 316 stainless steels, *Int J Frac* 101 (2000) 215–228.
- [21] R. Chaouadi, Crack resistance determination from the instrumented Charpy V-notched impact test, SCK•CEN Report (in preparation).
- [22] L. Tosal, G. Rodriguez, F.J. Belzunce, C. Betegon, The influence of specimen size on the fracture behavior of a structural steel at different temperatures, *J Test Eval* 28 (2000) 276–281.
- [23] T.L. Anderson, R.H. Dodds, Specimen size requirements for fracture toughness testing in the transition region, *J Test Eval* 19 (1991) 123–134.
- [24] K.C. Koppenhoefer, R.H. Dodds, Ductile crack growth in pre-cracked CVN specimens: numerical studies, *Nucl Eng Des* 180 (1998) 221–241.